

UCLA

UCLA Previously Published Works

Title

Cryo-EM reveals different coronin binding modes for ADP-and ADP-BeFx actin filaments

Permalink

<https://escholarship.org/uc/item/6zn1t2dj>

Journal

Nature Structural and Molecular Biology, 21(12)

ISSN

1545-9993

Authors

Ge, P
Durer, ZAO
Kudryashov, D
et al.

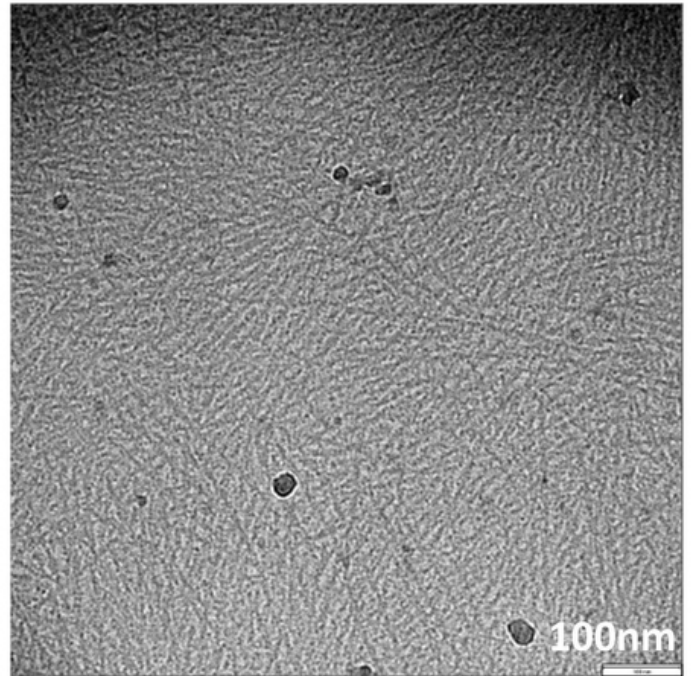
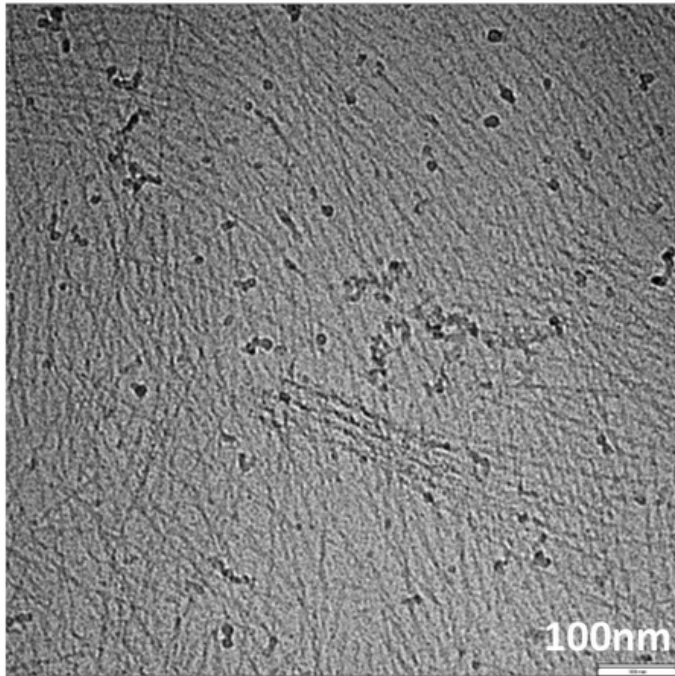
Publication Date

2014-12-11

DOI

10.1038/nsmb.2907

Peer reviewed

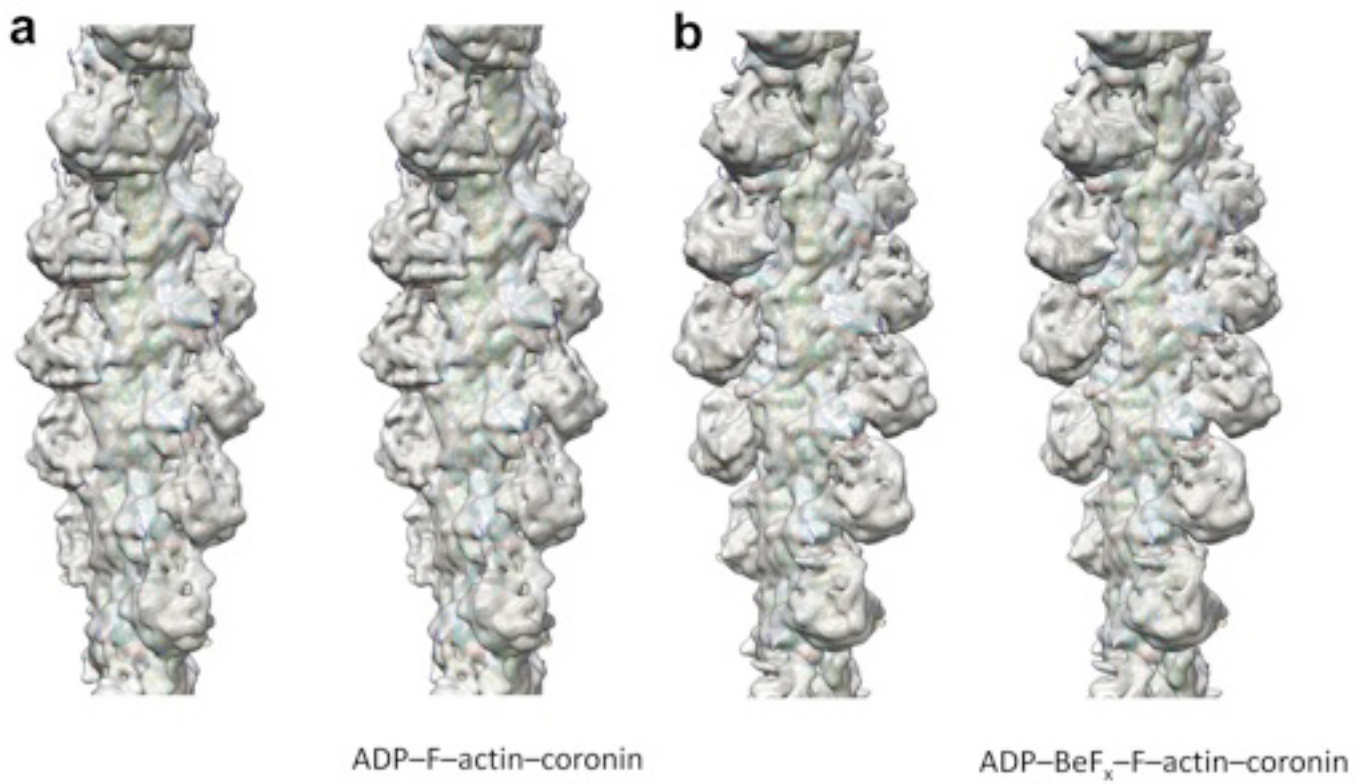


Supplementary Figure 1

Actin array generated by full-length coronin.

Representative cryoEM fields of full-length coronin decorated ADP-actin.

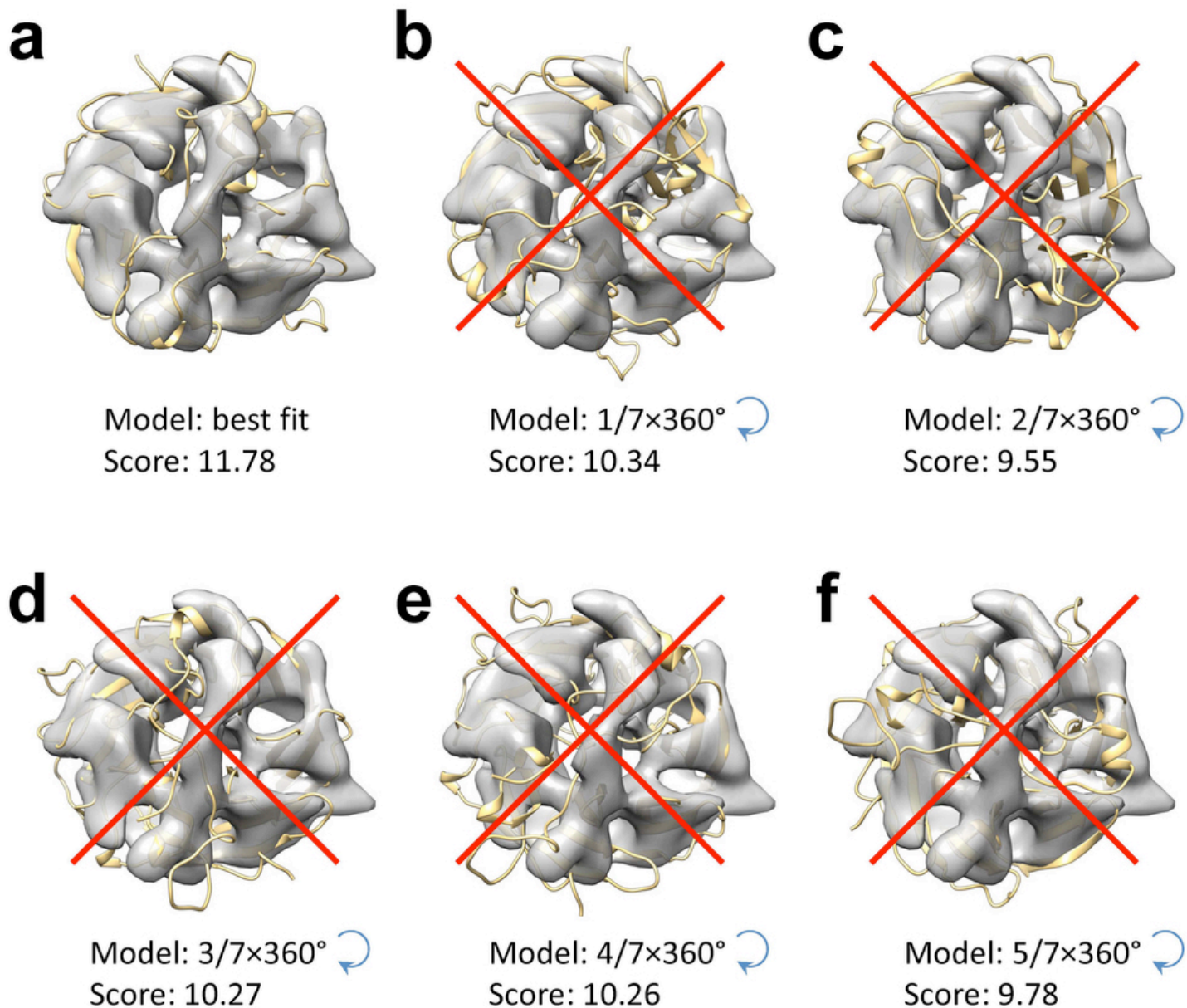
Full-length coronin bundles actin into thick bundles (left) and meshes (right). Bar: 100nm.



Supplementary Figure 2

Stereo views.

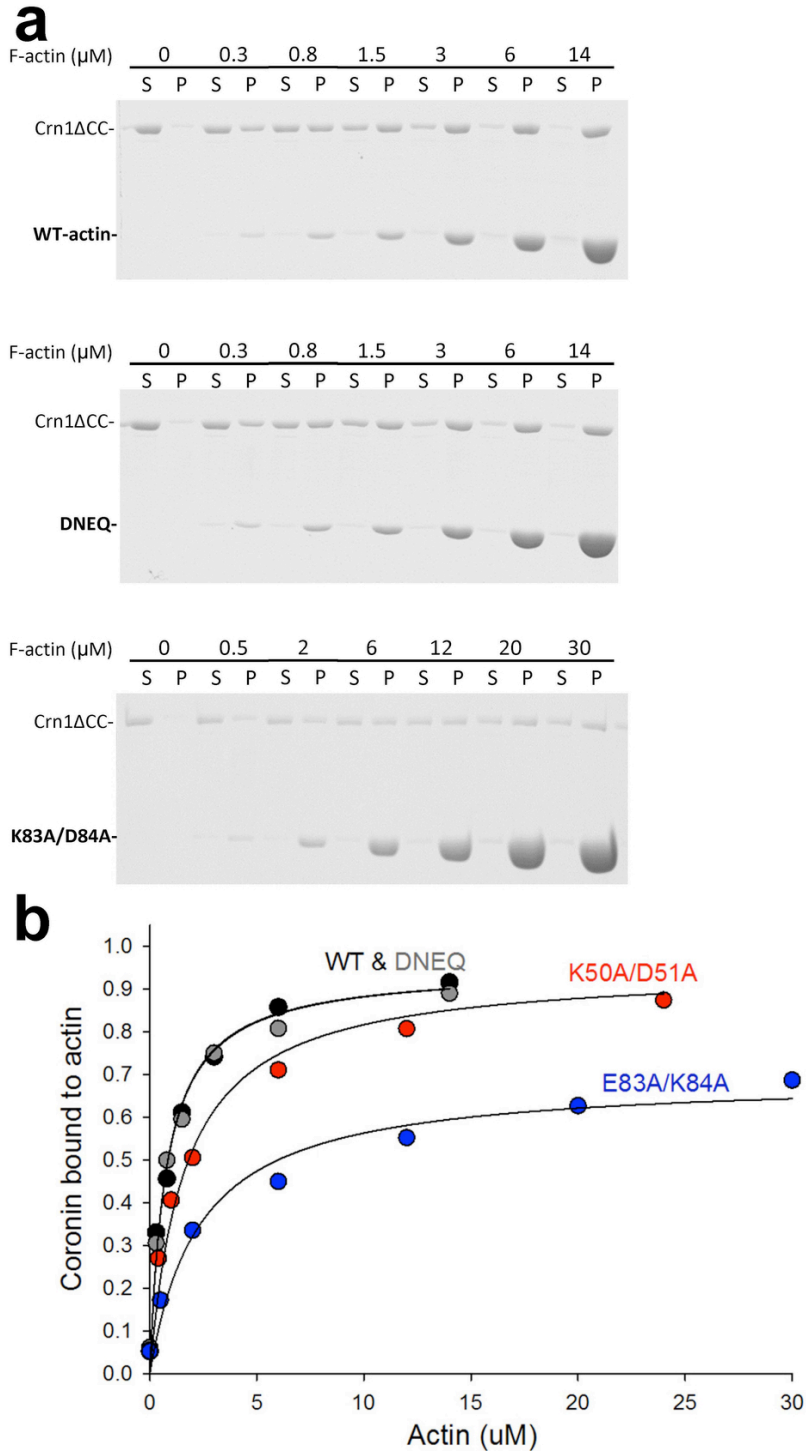
Stereo views of **Figure 1**, panels **b** and **f**.



Supplementary Figure 3

Comparison of all possible docking modes of the coronin density and its model.

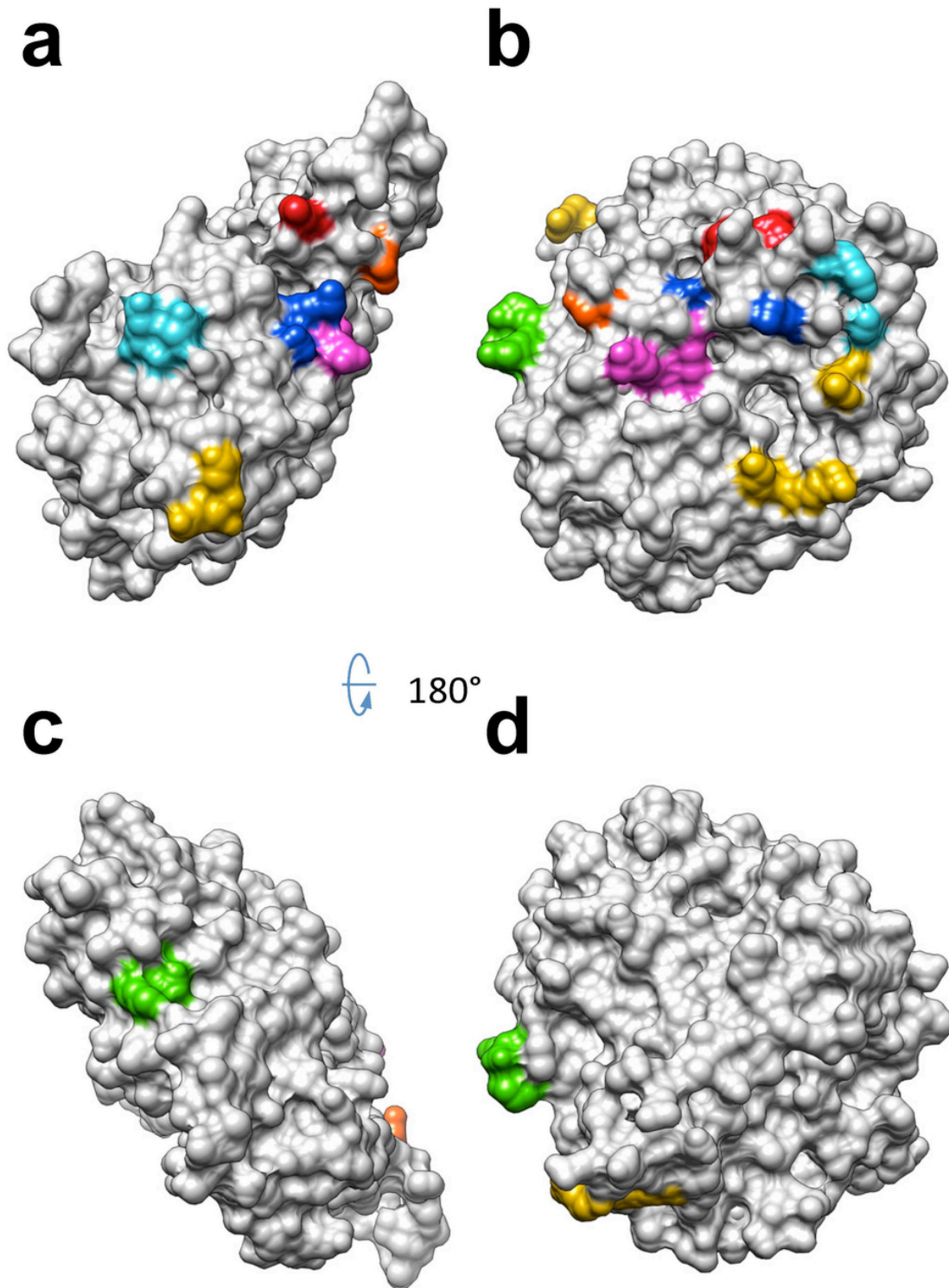
(a-f) The density corresponding to coronin in our ADP state structure is fitted with our homology model of coronin. Due to the pseudo-seven-fold symmetry of coronin's seven-bladed propeller, there are seven possible modes of docking. The docking that we chose in our paper (a) is significantly (>5 SD) better than other possible dockings. The last possible mode (model rotated by $6/7 \times 360^\circ$) cannot be generated, since the docking program automatically fits it towards the best model (a).



Supplementary Figure 4

Crn1 ΔCC binding to wild-type and mutant yeast ADP-actins.

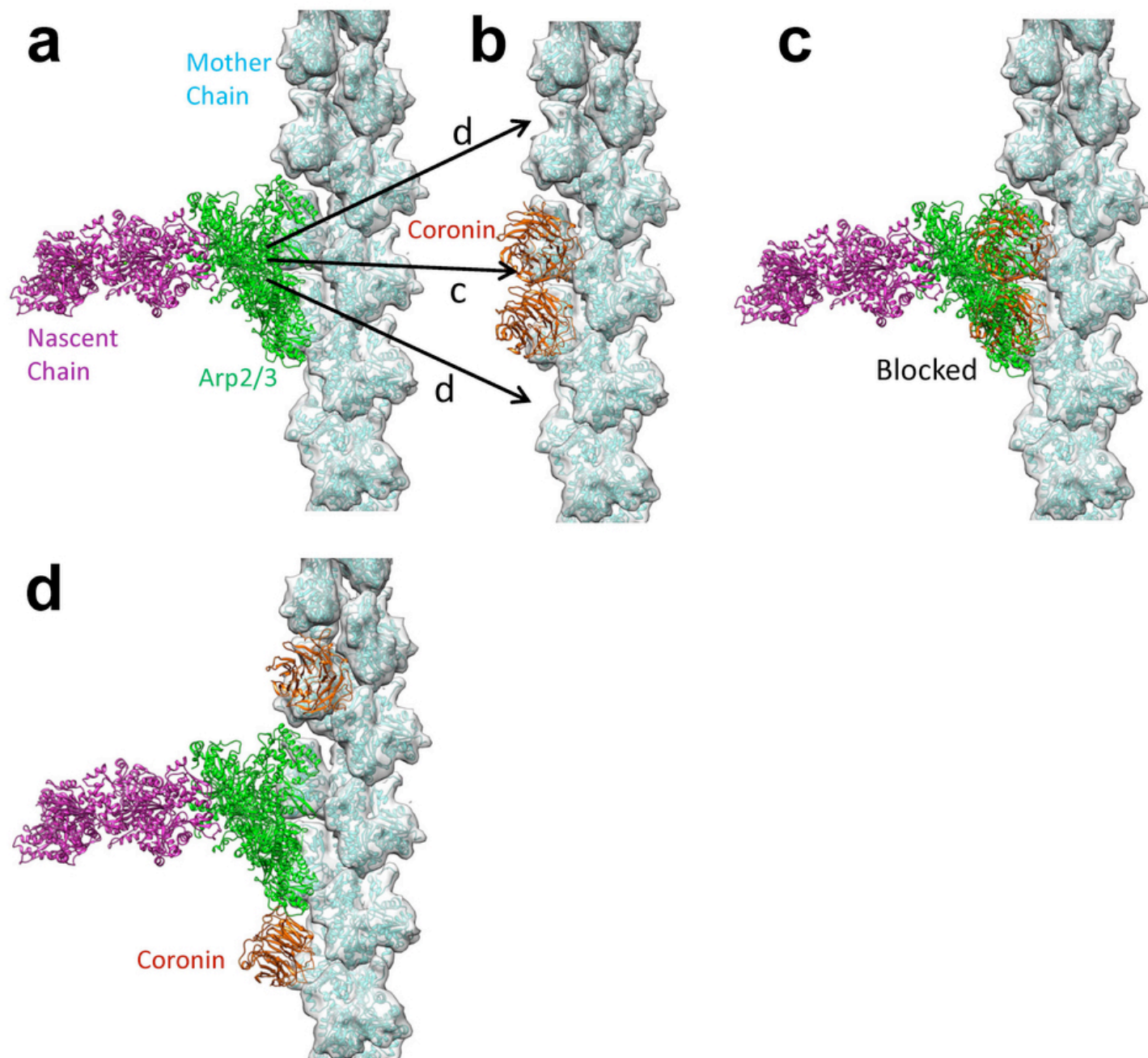
(a) Coomassie-stained gels of supernatant (S) and pellet (P) fractions of 1 μM Crn1 ΔCC cosedimented with 0-30 μM pre-polymerized wild type and mutant actins. **(b)** Quantification of Crn1 ΔCC binding by wild type and select mutant actins obtained for analysis of gels shown in **(a)**. Fractions of Crn1 ΔCC bound to various F-actins was determined by densitometry and plotted versus the concentration of F-actin.



Supplementary Figure 5

Distribution of key residues that mediate actin-coronin interaction.

Key residues that are shown in this study to be responsible for actin-coronin interaction are mapped on the surfaces of actin (**a, c**) and coronin (**b, d**). The key groups of interacting residues are colored as in Table 1, regardless of the interacting actin subunits.



Supplementary Figure 6

Competition between coronin and Arp2/3 complex at high coronin concentration.

The pseudo-atomic model of actin-Arp2/3 complex (**a**) is superimposed with that of ADP-F-actin-coronin, similarly to **Figure 6**. (**b**) Relative position of coronin in the superimposed model (the actin model from the actin-Arp2/3 complex is shown to simplify the comparison). (**c-d**) Coronin blocks binding of Arp2/3 complex at high coronin concentrations, when Arp2/3 complex and coronin compete for actin binding (**c**), but allows binding of Arp2/3 complex to adjacent unoccupied actins (**d**) at low coronin concentrations. In all panels, actin subunits are delineated by grey transparent surfaces derived from their atomic models.

Supplementary Table 1: Corresponding actin and coronin mutations

<i>Crn1</i> alleles with no detectable F-actin binding ²⁵	<i>Crn1</i> residues mutated to alanine	Charged actin residues within 8Å proximity	Actin mutants used in this study
Crn1-2	K10 R12	E361, D363, E364	D363A E364A
Crn1-6	R141 K142	E125, D363, E364	D363A E364A
Crn1-13	K295 D297	D80, D81, E83, K84	D80A D81A E83A K84A
Crn1-17	E320 R323	R37, R39, K50, D51, K68, D80, D81, K84	R37A R39A K50A D51A D80A D81A E83A K84A
Crn1-19	R361 R362, E364 E365	E361, D363, E364,	D363A E364A